THE ASTROPHYSICAL JOURNAL, 523:444–449, 1999 September 20

KINEMATIC MEASUREMENTS OF POLAR JETS OBSERVED BY THE LARGE-ANGLE SPECTROMETRIC CORONAGRAPH

B. E. WOOD AND M. KAROVSKA
Harvard-Smithsonian Center for Astrophysics, 60 Garden Street, Cambridge, MA 02138

AND

J. W. COOK, R. A. HOWARD, AND G. E. BRUECKNER[1]
E. O. Hulburt Center for Space Research, Naval Research Laboratory, Washington, DC 20375
Received 1998 December 4; accepted 1999 May 8

ABSTRACT

We analyze polar jets observed by the Large-Angle Spectrometric Coronagraph (LASCO) instrument aboard the *Solar and Heliospheric Observatory*. The events studied here are from 1997 March 24 and August 5. The main objective of our analysis is to determine whether the jets' motions are consistent with ballistic behavior. Although ballistic trajectories have some success in fitting the observed kinematic motions, there is substantial evidence that gravity alone is not regulating the movement of the jets. First of all, the August 5 events appear to exhibit slight accelerations rather than decelerations above 3 $R_\odot$. Second, all the events studied here have very similar velocities, suggesting that by the time the jets reach the LASCO field of view, the jets have been incorporated into the ambient solar wind. If this is the case, the jets could be very useful as tracers of the solar wind at low heights in the Sun's polar regions.

Subject headings: Sun: activity — Sun: corona

1. INTRODUCTION

White-light coronal images taken by the Large-Angle Spectrometric Coronagraph (LASCO) aboard the *Solar and Heliospheric Observatory* (*SOHO*) have revealed a new type of solar ejection phenomena called "polar jets." As seen in LASCO's C2 coronagraph, which images the corona from about 2 to 6 $R_\odot$, the jets appear as narrow, radially extended intensity enhancements that move outward from the Sun's polar regions in a nearly radial direction at speeds of about 125–350 km s^{-1} (St. Cyr et al. 1997; Wang et al. 1998). In the 3.5 yr since its launch, LASCO has detected about 3–4 of these jets per day.

The LASCO polar jets join a long list of jetlike phenomena observed on the Sun. This list includes spicules, macrospicules, and surges, which are all observable from the ground in Hα images and are visible at higher temperatures in lines such as He II λ304 (Beckers 1972; Roy 1973; Bohlin et al. 1975; Karovska & Habbal 1994; Suematsu, Wang, & Zirin 1995). There are also spectroscopically identified jets such as the chromospheric jets and explosive events seen by the High Resolution Telescope and Spectrograph rocket experiments (Brueckner & Bartoe 1983; Dere, Bartoe, & Brueckner 1983, 1989). Data from *Yohkoh* show that jet phenomena are also seen in X-rays (Shibata et al. 1992; Shimojo et al. 1996).

The degree to which these types of jets are interrelated is still not entirely clear. The X-ray jets, for example, are often associated with Hα surges, but not always (Shibata et al. 1992; Canfield et al. 1996). The chromospheric jets of Dere et al. (1983) are probably an EUV spectroscopic manifestation of spicules. The LASCO polar jets are often associated with EUV jet events seen near the solar surface by the Extreme-Ultraviolet Imaging Telescope (EIT) on *SOHO* (Moses et al. 1997; Wang et al. 1998).

Another issue concerns the acceleration mechanism of the jets. It is important to discern observationally whether the acceleration is impulsive or continuous. Continuous acceleration would be consistent with certain wave or multiple shock models, such as those that have been developed to explain spicules (see, e.g., Hollweg 1982; Hollweg, Jackson, & Galloway 1982; Sterling & Mariska 1990). Impulsive acceleration would suggest that single shocks or magnetic reconnection are more likely formation mechanisms (see, e.g., Suematsu et al. 1982; Cheng 1992; Shibata et al. 1992). In contrast to Wang et al. (1998), who only estimated average velocities for the jets in the C2 field of view, we will measure the precise height-versus-time behavior for a smaller sample of jets to see if their motions are consistent with simple gravitational deceleration, which would imply impulsive acceleration, or if continuous acceleration must be invoked to explain their trajectories. Our principal assumption is that we are observing plasma ejected into the solar gravitational field, rather than wave-related intensity enhancements.

2. OBSERVATIONS

2.1. *The LASCO and EIT Instruments*

The LASCO instrument consists of three different coronagraphs, which observe different height ranges in the solar corona. The internally occulted C1 coronagraph has the innermost field of view, ranging from 1.1 to 3 $R_\odot$. This coronagraph contains a tunable Fabry-Perot interferometer, which is used to image the corona in one of several coronal emission lines available in the optical wavelength regime. The C2 and C3 coronagraphs are both externally occulted, broadband, white-light coronagraphs, with C2 observing heights from 2 to 6 $R_\odot$ and C3 covering the outer corona from 4 to 32 $R_\odot$. Brueckner et al. (1995) provide a full description of LASCO and its capabilities. Polar jets are rarely detected by the C1 and C3 coronagraphs, so we present only C2 data here. We focus on jets detected in two sequences of C2 images, one from 1997 March 22–24 and the other from 1997 August 5–6.

For the 1997 August 5–6 sequence we will analyze EIT observations in addition to the LASCO data. The EIT

[1] We are saddened to report that our colleague Guenter E. Brueckner died 1998 July 11.

instrument, which is described in detail by Delaboudinière et al. (1995), images the Sun in one of several EUV bandpasses. The EIT images used here are in the bandpass centered on the Fe XII 195 Å line, which is the bandpass most frequently used for EIT's solar monitoring program.

2.2. *The 1997 March 22–24 Observing Sequence*

On 1997 March 22 at 23:46 UT, a unique sequence of LASCO C2 images of the north polar region was begun which lasted for about 41 hr. The average time between the 200 images taken during the sequence was 12.2 minutes, an improvement of about a factor of 2 over the time cadence normally attained by LASCO in its monitoring of the solar corona. The 100 s exposure times of the images in this sequence are also improvements over the standard C2 synoptic data, being about a factor of 4 higher than normal.

This sequence was designed to study polar outflows in general. However, such studies are complicated by the existence of foreground material in the streamer belt, especially when high-latitude streamers rotate into the polar field of view. The most obvious example of this in our data is a bright radial front of enhanced intensity in the northeast quadrant, which advances slowly northward while remaining oriented in a radial direction. Inspection of LASCO data obtained in the days before and after the 200 image sequence demonstrates that this is a bright, high-latitude streamer that becomes superimposed onto the Sun's north polar region after rotating into the foreground. The existence of this foreground material is a serious complication for studies of polar plumes because it is not easy to separate the intensities of the bright plumes from those of the foreground streamer material.

Bright polar jets, however, are easily discerned in C2 data, and the association of many of these events with EUV events seen near the polar limbs of the Sun confirms they do emanate from the poles (Wang et al. 1998). On March 24, near the end of the polar imaging sequence, a series of three jets is seen originating from the same location near the north pole, appearing at 7:03, 10:08, and 12:00 UT, respectively. In order to see the jets clearly, we remove as much as possible any radial intensity gradients from the C2 images by computing an average of the 200 images and subtracting it from each individual image. Figure 1 shows four resulting images of the first and brightest of the three jets.

In order to study the jets further, we focused our attention on a thin sector centered on the axis of the jets. We partitioned the sector into 72 segments and then measured intensities along the axis of the sector by summing the pixels within these segments. In Figure 2, we display the evolution of these intensity tracings with time for the brightest of the three jets. This pseudoimage has been smoothed to improve its appearance. The axis of the jets is not precisely radial, but it is instead at an angle such that an extension of the axis passes well above Sun center rather than going through it. This is not a surprise, since polar plumes show similar superradial expansion (DeForest et al. 1997). For the y-axis of Figure 2, we have made the nonlinear conversion from distance along the jet axis to distance from Sun center. To be more precise, the heliocentric distance, R, is computed from the equation

$$R^2 = r^2 + x^2 - 2xr \cos \phi , \tag{1}$$

where ϕ is the obtuse angle between the jet axis and the solar rotation axis, r is the distance of the jet's centroid from

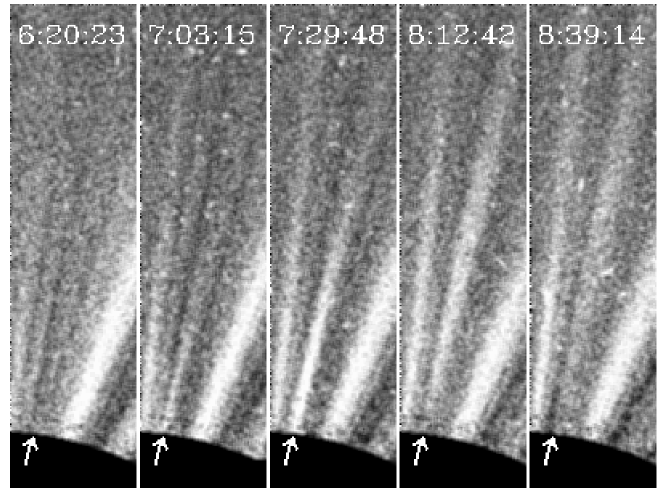

FIG. 1.—Series of LASCO C2 images from 1997 March 24 showing a bright polar jet near the north pole

the rotation axis as measured along the jet axis, and x is the distance between Sun center and the intersection between the jet and solar rotation axes.

The numerous jets analyzed by Wang et al. (1998) are also superradial with larger superradial expansion factors for jets that are further from the poles, once again consistent with polar plume behavior. Note that the apparent universality of this behavior demonstrates that the jets are all ejected nearly in the plane of the sky without a broad distribution of ejection angles, meaning we do not have to concern ourselves with projection effects.

For the brightest two jets, we have estimated where the centroids of the jets are located by fitting Gaussians to each intensity tracing where the jets are fully visible. These centroid measurements are displayed as black circles in Figure 3 and are shown with the 2 σ error bars provided by our Gaussian fitting procedure. For the brightest jet, the centroid measurements are also shown in Figure 2, along with the upper $1/e$ points of the Gaussians (*yellow circles*), which provide estimates for the leading edge of the jet. Cruder estimates of the leading edge locations are made by eye for several additional images. For these images too much of the jet intensity profile is obscured by the C2 occulter for a Gaussian fit to be performed. For the last and faintest jet, we do not attempt any of these measurements, since this jet is blended somewhat with the second jet and fades quicker than the other two jets.

The centroid and leading edge curves in Figures 2 and 3 show decreasing slopes with time, indicating decelerations. Most of the polar jets analyzed by Wang et al. (1998) also show evidence for substantial deceleration between their initiation times and when they enter the C2 field of view. This behavior is different from that of coronal mass ejections, which generally show continuous acceleration below 3–4 $R_\odot$ (Dere et al. 1997; Wood et al. 1999). The simplest possible interpretation for the deceleration seen for the polar jets is that it is due to gravity.

We have fitted the centroid data points in Figure 3 with ballistic trajectory curves to test this simple interpretation of the jets' kinematic behavior. (For the brightest jet, the fit is also shown in Fig. 2.) The centroid curves are simple enough that a quadratic or even linear polynomial could

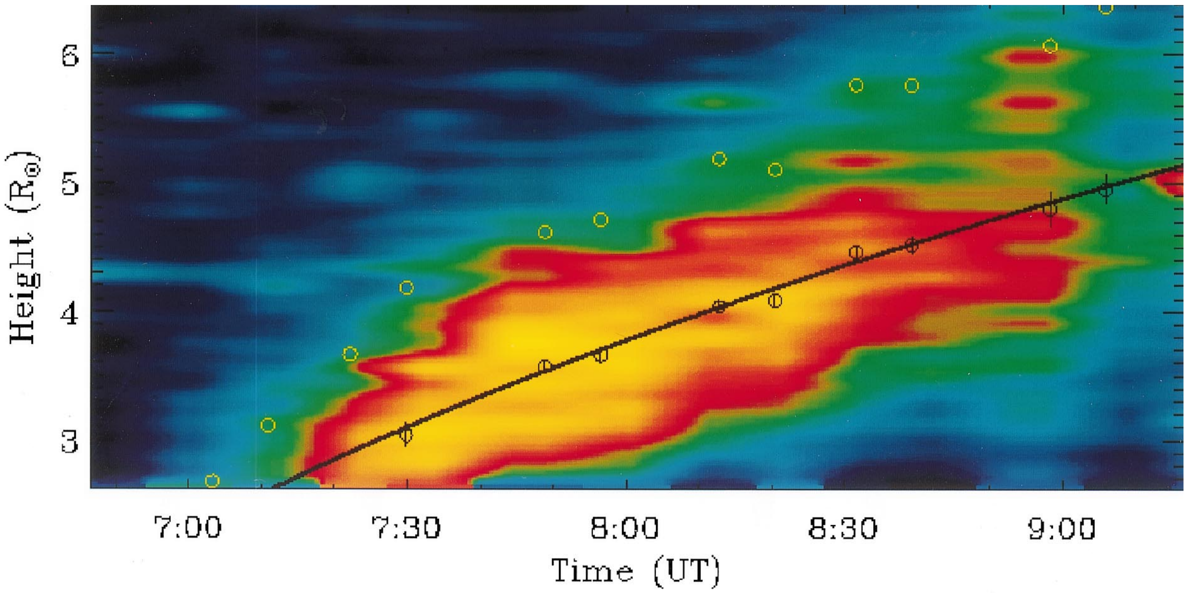

FIG. 2.—Sequence of intensity tracings from LASCO C2 images along the axis of the polar jet in Fig. 1. This pseudoimage has been smoothed for the sake of clarity. For each tracing, we identify a centroid (*black circles*) and leading edge (*yellow circles*) for the jet using Gaussian fits. The centroid measurements are fitted with a ballistic trajectory (*black line*).

also be used to fit the data, but a ballistic curve is a more physical model. A ballistic trajectory would be a simple parabola close to the Sun, but we observe the jets well above the solar surface, where the $1/r^2$ height dependence of the gravitational deceleration is important. Assuming the jet material is ejected at $r_0 = R_\odot$ with an initial velocity v_0, the differential equation for the trajectory is

$$\frac{dr}{dt} = \left[v_0^2 - 2g_\odot\ R_\odot\left(1 - \frac{R_\odot}{r}\right)\right]^{1/2}, \tag{2}$$

where $g_\odot = 0.274$ km s^{-2} is the gravitational deceleration constant at the Sun's surface. We solve this equation numerically using a fourth-order Runge-Kutta technique (Press et al. 1989).

Our best fits to the data are shown in Figure 3. These curves fit the data nicely, demonstrating that the motions of the two jets are consistent with ballistic trajectories. For the first jet, the curve implies a decrease in velocity from 292 km s^{-1} at 3 $R_\odot$ to 184 km s^{-1} at 5 $R_\odot$. The initial ejection velocity of this jet is $v_0 = 584 \pm 4$ km s^{-1}. Note that the actual velocity will be somewhat lower if the ejection occurs well above the solar surface. The initial velocity is slightly below the Sun's escape velocity of 619 km s^{-1}, suggesting that in the absence of other forces the jet material will fall back toward the Sun after reaching a height of 9.0 $R_\odot$. Unfortunately, the jet fades before we can tell if this actually occurs. Note that the jet was not detected at all in images from the C3 coronagraph, which has a larger field of view (4–32 $R_\odot$) and greater sensitivity than C2, but with much lower spatial and time resolution.

The results for the second jet are similar (see Fig. 3*b*), with a somewhat lower ejection velocity of $v_0 = 551 \pm 5$ km s^{-1}. In the absence of other forces, the jet material would reach a height of 4.8 $R_\odot$ before falling back to the Sun, but as in Figure 2, the jet dissipates well before reaching this point.

The leading edge curves in Figure 2 are *not* well fitted by ballistic trajectories, because they exhibit too much deceleration as they enter the C2 field of view. However, it is unclear if this failure has any physical meaning. There is no sharp leading edge to the polar jets, and the $1/e$ point where we chose to define the leading edge location is arbitrary. Unlike the centroid, the location of the leading edge as defined by the $1/e$ point will be affected both by expansion

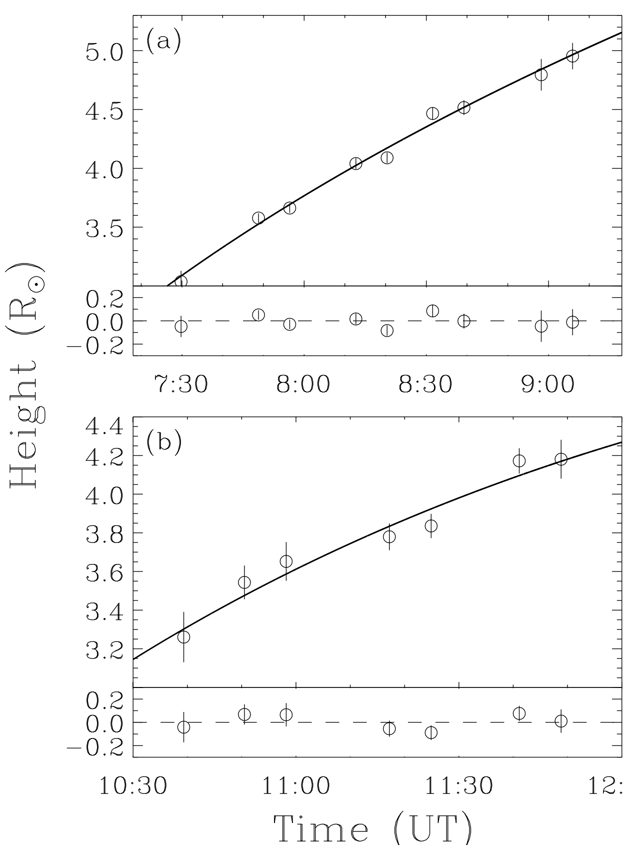

FIG. 3.—(*a*) Centroids (*circles*) and fitted ballistic trajectory curve for the first and brightest March 24 jet reproduced from Fig. 2, along with residuals of the fit. (*b*) Centroid measurements (*circles*) and fitted ballistic trajectory curve for the second March 24 jet.

or contraction of the jet and by its overall brightening or dimming. Thus the motion of the centroid is more relevant to discussions of the jets' true kinematical behavior.

Figure 3 shows that with C2 data alone we can track the centroid of the jet through only a small portion of the suggested ballistic trajectory. Thus the success of the ballistic trajectory in fitting the data is far from being a clear demonstration of ballistic behavior. The centroids can also be fitted reasonably well with a straight line, although not quite as well as with the trajectories in Figure 2. The test of the ballistic hypothesis could be strengthened if the initiation time of the jet could be pinned down by EIT observations. However, despite the improved signal-to-noise ratio and time resolution of the March 22–24 C2 observing sequence, these data do have the one major drawback that there are no EIT data available at that time for comparison. In order to see if including EIT data can better resolve the issue of whether the motions of jets are ballistic or not, we now look at a few jets that were seen by both LASCO and EIT on 1997 August 5–6.

2.3. *The 1997 August 5–6 Polar Jets*

Wang et al. (1998) collected a sample of 27 LASCO polar jets that were clearly associated with EIT events. This sample includes two bright jets from 1997 August 5. These two jets were in fact part of a sequence of six polar jets that originated from the same location near the Sun's north pole within a 19 hr time span on August 5–6. Given the multiplicity of events and the better-than-average time resolution of the C2 data taken at that time, we decided the August 5–6 jets would be the best events from the sample of Wang et al. (1998) for us to analyze kinematically.

We processed the data in much the same way as we did for the March 22–24 data. In Figure 4 we show the intensity tracings along the axis of the six jets and identify the jets with numbers. The dark rectangles at the top of the image are caused by the truncation of the field of view of many of the C2 images, which is a consequence of *SOHO*'s limited telemetry rate. The two brightest jets in Figure 4 (jets 2 and 5) are the ones identified by Wang et al. (1998) as having accompanying EIT events. A detailed inspection of the EIT Fe XII λ195 images reveals that all six of the jets are in fact accompanied by EUV jets near the solar surface. This suggests that *all* LASCO polar jets may have associated EUV events, but a much larger sample would be necessary to demonstrate this.

Figure 5 shows the EUV jet associated with polar jet 4. In constructing this sequence of images, we computed an average image from all the August 5 EIT data, and we then subtracted this average from the individual images. The faint EUV jet is visible in the second panel of Figure 5. This event is typical in that the EUV jet is clearly detected in just one EIT image, and it is a narrow, radially extended feature roughly analogous to its white-light appearance in the LASCO C2 field of view. The EUV jets are similar in appearance to macrospicules, suggesting the possibility that they are in fact just very fast and energetic macrospicules. The exception is the brightest jet (jet 2). The EUV jet associated with this event is a substantially broader and brighter eruption (see Fig. 3 in Wang et al. 1998). It is interesting that this difference of appearance in EIT data does not manifest itself in a fundamentally different white-light appearance in LASCO C2 data. We also note that the brightest LASCO jets are not necessarily associated with the brightest EUV jets. After jet 2, which is clearly the brightest for both LASCO and EIT, the most dramatic EUV events are those associated with jets 1 and 3, jets that are not very bright in C2 data (see Fig. 4).

For the three polar jets that are brightest in the LASCO data, we perform the same kinematic analysis that was done for the March 24 jets. The results are shown in Figure 6. As described above, each jet has an associated EUV event detected in a single EIT image. We estimate the centroid of the EUV jet by eye, providing us with the earliest data points for the height-versus-time curves in Figure 6. The spatial correspondence of the jets white-light intensities with its EUV emission is uncertain, so we assign generous error bars to the EIT data points in Figure 6. However, the EIT field of view only extends to about 1.4 $R_{\odot}$, so merely restricting the centroid to be somewhere in the EIT image would be enough to significantly constrain the initiation time of the jet.

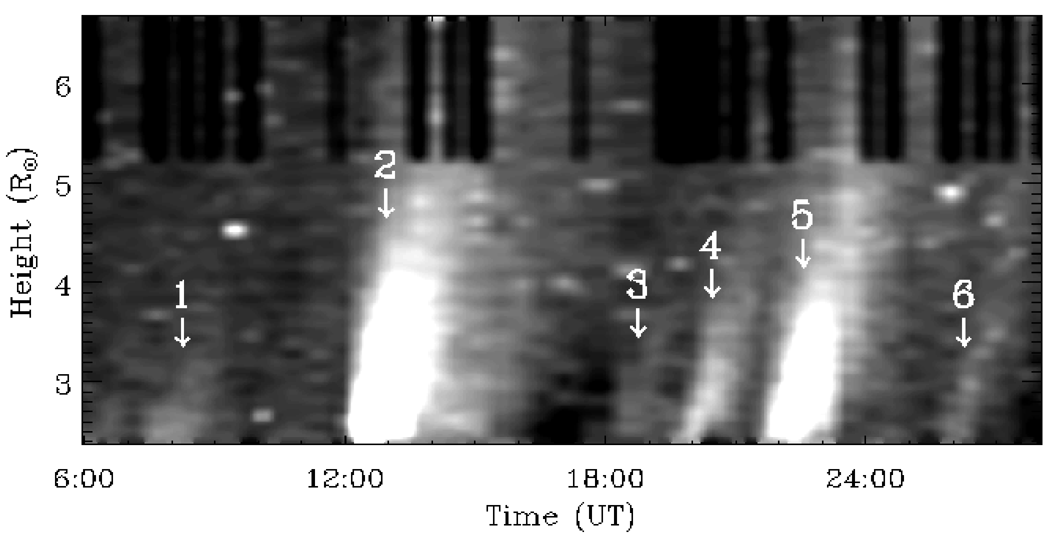

FIG. 4.—Series of intensity tracings from LASCO C2 images along the axis of a sequence of 6 polar jets from 1997 August 5–6, which are numbered in the figure. The intensities have been smoothed for the sake of clarity. The field of view of some of the C2 images was truncated because of *SOHO*'s limited telemetry rate, which is the reason for the numerous dark rectangles at the top of the image.

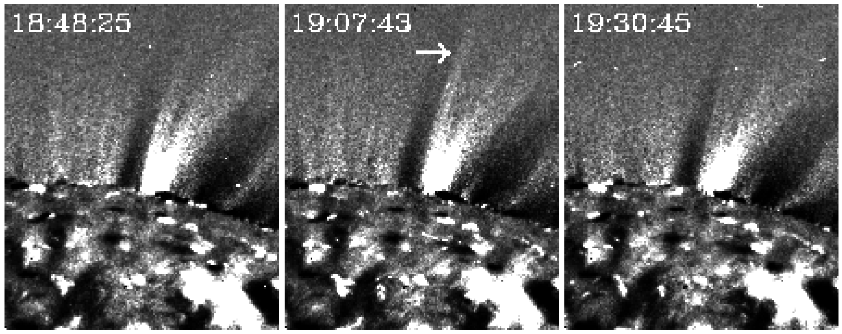

FIG. 5.—Sequence of three EIT Fe XII λ195 images from 1997 August 5, after subtraction of an average image computed from that day's observations. The EUV jet associated with polar jet 4 (see Fig. 4) is visible in the second panel.

For each of the three jets, the first three data points suggest significant deceleration at low heights, which is consistent with the kinematic scenario of impulsive acceleration followed by gravitational deceleration. Furthermore, the three ballistic trajectories in Figure 6 demonstrate some ability to fit the data, with initial velocities of 545 ± 4, 545 ± 4, and 571 ± 1 km s^{-1}, respectively. However, there are significant discrepancies between the fits and the data, especially for jet 4 (see Fig. 6*b*). The primary reason for the discrepancies is that for all three jets the C2 data points by themselves actually seem to show positive curvature above 2.5 $R_\odot$ rather than negative, suggesting slight accelerations rather than decelerations.

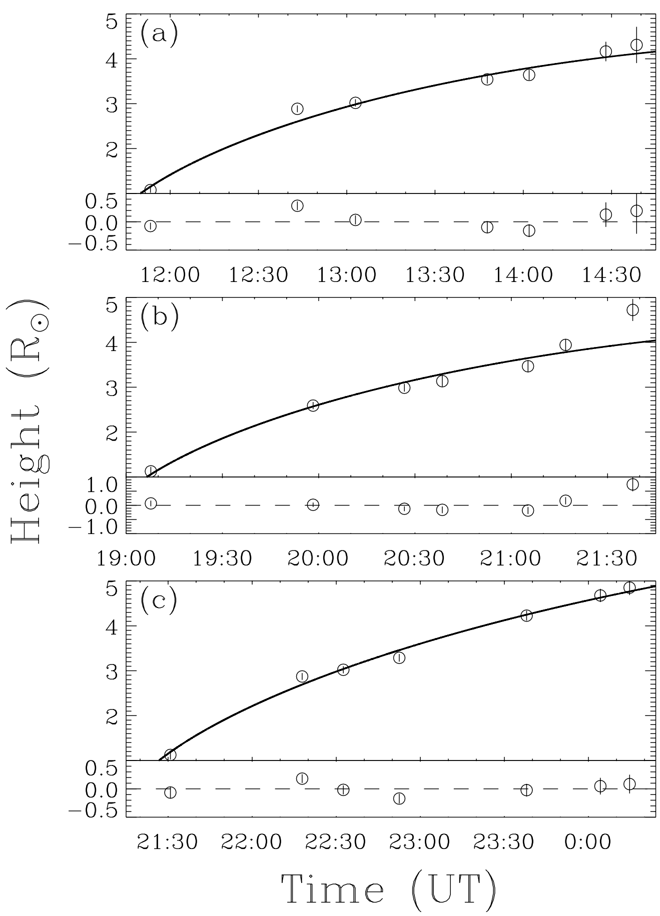

FIG. 6.—(*a*) Centroids of polar jet 2 in Fig. 4 (*circles*) measured using Gaussian fits to the intensity tracings. The jet is detected by EIT, which provides an additional centroid measurement at low heights below the C2 field of view. The centroid measurements are fitted with a ballistic trajectory (*solid line*), and residuals of the fit are displayed below the main figure. (*b*) Same as (*a*), but for jet 4. (*c*) Same as (*a*), but for jet 5.

3. DISCUSSION

As described above, the polar jets are generally radially extended structures in EIT images as well as in the C2 data. This implies that the material is ejected over some period of time and not all at once. If the jets are ejected with a broad distribution of velocities, one would expect to see a substantial lengthening of the jets in the C2 images. Thermal speeds for protons at coronal temperatures are about 100 km s^{-1}, which is of the same order as the jet velocities observed in the C2 data. Thus one might also expect to see a lengthening of the jets due simply to thermal expansion, in the absence of any force confining the jet material.

Three of our five jets show some evidence for lengthening, and in Figure 7 we plot the FWHM of our Gaussian fits to these jets' intensity profiles as a function of height. The FWHM of these jets increases by about 0.5–1.0 $R_\odot$ during their roughly 90 minute passage through the C2 field of view, suggesting expansion velocities of 65–130 km s^{-1}. This value is roughly consistent with the coronal thermal speed quoted above, so perhaps the observed lengthening is due to thermal expansion. The two jets that do not show

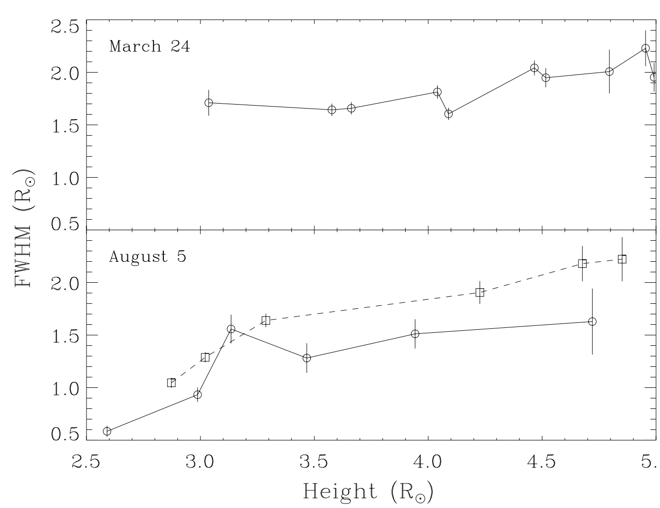

FIG. 7.—For the three polar jets in our sample that show evidence for lengthening in the LASCO C2 field of view, the FWHM of the Gaussians fitted to their intensity tracings are plotted versus centroid height. The top panel is for the first and brightest jet from 1997 March 24, and the bottom panel is for jets 4 and 5 from August 5 (*solid and dashed lines, respectively*).

any obvious lengthening are the second March 24 jet and jet 2 from August 5. The centroids of these jets are tracked through smaller height ranges than the other three jets, and the uncertainties in the measured FWHM are also higher, which might explain the absence of any detectable lengthening for these jets.

In the simplest impulsive acceleration scenarios for jets, gravity is expected to be the dominant force on the jet following the initial acceleration, especially in the Sun's polar regions, where the open magnetic fields should not significantly impede the jet's motion. Much effort has been made to see if spicules and macrospicules follow the ballistic trajectories that would provide support for this scenario, but the results are not conclusive. The motions of some events do seem to be ballistic, especially near the tops of their trajectories, and the lengths and lifetimes of spicules appear to be related in a manner consistent with ballistic behavior (Nishikawa 1988; Suematsu et al. 1995). However, the motions of many other events appears to be non-ballistic, and the large initial velocities of up to 70 km s^{-1} required for ballistic spicules to reach their maximum heights are not observed (Suematsu et al. 1995).

Macrospicules, on the other hand, have been found to have velocities of 100–150 km s^{-1} (see, e.g., Karovska & Habbal 1994). This is still much lower than the 540–590 km s^{-1} initial velocities we have measured for the polar jets. Material motions of up to 400 km s^{-1} are occasionally seen during transition region explosive events (Brueckner & Bartoe 1983; Dere et al. 1983, 1989). However, the only reported jet velocities that we are aware of that actually match or exceed those of the polar jets are for a few of the fastest X-ray jets, which can reach speeds of 1000 km s^{-1} (Shimojo et al. 1996).

The LASCO polar jets appear to show significant deceleration at low heights, but ballistic trajectories do not appear to be entirely successful in fitting the motions of the August 5 jets in the C2 field of view, implying that gravity may not be the only force acting on the jets. The velocities of the fitted ballistic trajectories provide another argument against purely ballistic motion. The average velocities of the five jets presented here in the C2 field of view are all in the range 125–230 km s^{-1}, and the ballistic trajectories shown in Figures 3 and 5 suggest initial velocities in a narrow range of 540–590 km s^{-1}.

In the gravitational deceleration scenario, jets with initial velocities below about 500 km s^{-1} will never reach the C2 field of view, so explaining the lower initial velocity limit is not a problem. The upper limit, however, *is* hard to explain. If the impulsive acceleration followed by gravitational deceleration scenario is true, why are there no jets with initial velocities greater than 620 km s^{-1} and velocities in the C2 field of view greater than 300 km s^{-1}? Is it possible that for some reason jets with high velocities do not have sufficient brightness to be observable with LASCO?

The rather homogeneous kinematic behavior of the polar jets suggests that by the time the jets reach the C2 field of view, their motions are simply those of the ambient solar wind outflow. This is consistent with the findings of Wang et al. (1998), who also noted the homogeneous kinematic behavior of the jets. The jet velocities do appear to be roughly consistent with the polar outflow velocities measured between 1.5 and 4.0 $R_{\odot}$ by the Ultraviolet Coronagraph Spectrometer instrument on *SOHO* (Kohl et al. 1998). If the polar jets are just following the general wind outflow in the C2 field of view, then they must be decelerated by interactions with the wind shortly after their ejection. Future investigations will focus on the nature of this implied drag force. For example, there is the question of whether Coulomb collisions at coronal densities provide enough of a drag force to decelerate the jets, or whether there is a stronger force present, possibly electromagnetic in nature.

If the polar jets are just following the general wind outflow, the kinematic behavior of the jets unfortunately cannot be used to infer much about their ejection mechanism. However, in this scenario the jets could prove to be very useful as tracers for the high-speed wind in coronal holes.

This project is supported by funding from the Naval Research Laboratory to the Harvard-Smithsonian Center for Astrophysics under contract N0014-97-1-G023. M. K. is a member of the *AXAF* Science Center, which is operated under contract NAS8-39073 and is partially supported by NASA. G. E. B., J. W. C., and R. A. H. are supported by NASA and the Office of Naval Research. LASCO is a cooperative project of an international group of scientists at the Naval Research Laboratory, Washington, D.C., the Max-Planck Institut für Aeronomie, Germany, the Laboratoire d'Astronomie Spatiale, France, and the Space Research Group at the University of Birmingham, England. *SOHO* is a project of international cooperation between ESA and NASA.

REFERENCES

Beckers, J. M. 1972, ARA&A, 10, 73
Bohlin, J. D., Vogel, S. N., Purcell, J. D., Sheeley, N. R., Jr., Tousey, R., & Van Hoosier, M. E. 1975, ApJ, 197, L133
Brueckner, G. E., & Bartoe, J.-D. F. 1983, ApJ, 272, 329
Brueckner, G. E., et al. 1995, Sol. Phys., 162, 357
Canfield, R. C., Reardon, K. P., Leka, K. D., Shibata, K., Yokoyama, T., & Shimojo, M. 1996, ApJ, 464, 1016
Cheng, Q.-Q. 1992, A&A, 266, 537
DeForest, C. E., Hoeksema, J. T., Gurman, J. B., Thompson, B. J., Plunkett, S. P., Howard, R., Harrison, R. C., & Hassler, D. M. 1997, Sol. Phys., 175, 393
Delaboudinière, J.-P., et al. 1995, Sol. Phys., 162, 291
Dere, K. P., Bartoe, J.-D. F., & Brueckner, G. E. 1983, ApJ, 267, L65
———. 1989, Sol. Phys, 123, 41
Dere, K. P., et al. 1997, Sol. Phys., 175, 601
Hollweg, J. V. 1982, ApJ, 257, 345
Hollweg, J. V., Jackson, S., & Galloway, D. 1982, Sol. Phys., 75, 35
Karovska, M., & Habbal, S. R. 1994, ApJ, 431, L59
Kohl, J. L., et al. 1998, ApJ, 501, L127
Moses, D., et al. 1997, Sol. Phys., 175, 571
Nishikawa, T. N. 1988, PASJ, 40, 613
Press, W. H., Flannery, B. P., Teukolsky, S. A., & Vetterling, W. T. 1989, Numerical Recipes (New York: Cambridge Univ. Press)
Roy, J.-R. 1973, Sol. Phys., 32, 139
Shibata, K., et al. 1992, PASJ, 44, L173
Shimojo, M., Hashimoto, S., Shibata, K., Hirayama, T., Hudson, H. S., & Acton, L. W. 1996, PASJ, 48, 123
St. Cyr, O. C., et al. 1997, in Proc. 31st ESLAB Symp. (ESA SP-415; Noordwijk: ESA), 103
Sterling, A. C., & Mariska, J. T. 1990, ApJ, 349, 647
Suematsu, Y., Shibata, K., Nishikawa, T., & Kitai, R. 1982, Sol. Phys., 75, 99
Suematsu, Y., Wang, H., & Zirin, H. 1995, ApJ, 450, 411
Wang, Y.-M., et al. 1998, ApJ, 508, 899
Wood, B. E., Karovska, M., Chen J., Brueckner, G. E., Cook, J. W., & Howard, R. A. 1999, ApJ, 512, 484